Clays and Clay Minerals, Vol. 67, No. 6:481–487, 2019

GIANT MULTISTEP CRYSTALLINE VS. OSMOTIC SWELLING OF SYNTHETIC HECTORITE IN AQUEOUS ACETONITRILE

Raphael Kunz, Sonja Amschler, Andreas Edenharter, Lina Mayr, Sebastian Herlitz, Sabine Rosenfeldt, and Josef Breu *

[1]Department of Chemistry and Bavarian Polymer Institute, University of Bayreuth, 95447 Bayreuth, Germany

Abstract—Intercalation of large organocations into 2:1 clay minerals may be hampered by two problems: on one hand, the solubility of organocations in water is limited and the resulting high selectivity for adsorption in the polar solvent may lead to non-equilibrium structures. On the other hand, the large expansion of the interlayer space will slow down kinetics of ion exchange considerably. The best workaround for these obstacles is to suspend the clay minerals in mixtures of water with more hydrophobic organic solvents that nevertheless trigger a considerable expansion of the interlayer space by swelling. This in turn fosters ion exchange. The current study, therefore, revisited pioneering work by Bradley (1945) and investigated the swelling behavior of synthetic sodium hectorite (Na-hec) as a function of the composition of the swelling solvent, a mixture of acetonitrile and water. Up to a maximum acetonitrile content of 65 vol.%, delamination by osmotic swelling occurred. At even higher acetonitrile concentrations, swelling was limited to the crystalline swelling regime where a step-like adjustment of the *d* value was observed. Several mixtures were identified yielding a well defined and uniform interlayer height as evidenced by rational 00*l*-series with the *d* spacing decreasing with increasing acetonitrile content. Surprisingly, for a specific acetonitrile:water ratio even an ordered interstratification of two strictly alternating interlayer heights with distinctly different solvent compositions was observed.

Key words—Crystalline swelling · Hectorite · Ordered interstratification · Osmotic swelling · Solvent mixtures

INTRODUCTION

The swelling behavior of clays in water is a well understood and well documented process (Norrish 1954; Madsen & Müller-Vonmoos 1989; Marry et al. 2011) and the structures at molecular resolution have been determined (Kalo et al. 2012). Swelling comprises two regimes, namely crystalline and osmotic swelling. The latter was shown more recently to actually consist of two sub-regimes with two distinct dependencies of silicate layer separation as a function of water content (Michot et al. 2006; Rosenfeldt et al. 2016): In the initial stages of swelling (regime one), a single phase gel (Wigner crystal) was formed with the separation of adjacent layers being proportional to (layer thickness)$\times\Phi^{-1}$, where Φ is the volume fraction of clay mineral. At later stages an inflection point was observed after which a nematic phase was observed and swelling increased at a slower pace (regime two). For synthetic hectorites and nontronites or montmorillonites (Michot et al. 2006) the transition between the two regimes occurs at different separations and the slope of the separation dependency in the second regime differs also. For all clay materials the general picture resembles early work by Viani et al. (1983) who, when measuring the osmotic pressure of montmorillonites, also observed an inflection point beyond which swelling no longer follows the Langmuir equation.

Crystalline swelling of clays is crucially influenced by the type of interlayer cation (Mooney et al. 1952; Möller et al. 2010), water activity (Hofmann et al. 1933; Devineau et al. 2006; Stöter et al. 2015), and the intensive variables temperature (Möller et al. 2010; Stöter et al. 2015) and pressure (You et al. 2013). Even the nature of the additional anion (OH^-, F^-) has some influence (Dazas et al. 2013). Experimental studies of the swelling behavior of natural clay minerals like montmorillonite are, unfortunately, obstructed by heterogeneities in charge density, leading to random interstratifications of various hydration states at any given relative humidity (r.h.) (Ferrage et al. 2005). Melt synthesis, as applied to synthetic fluorohectorite, yields much better charge homogeneity (Stöter et al. 2013). Consequently, the intracrystalline reactivity is uniform at all length scales (interlayer domain, tactoid, powder) which removes the need to deal with random interstratifications when interpreting diffraction patterns. The different hydration stages are compositionally and structurally (Kalo et al. 2012) well defined and are separated by plateaus of ranges of r.h. For $Na_{0.7}$ fluorohectorite in the two-layer hydration state, Na^+ is complexed by six water molecules that bridge the interlayer space through hydrogen bonding with defined phase. In the one-layer hydrate, Na^+ is surrounded by only three water molecules and the coordination is completed by six basal oxygens. For $Na_{0.5}$ fluorohectorite (Na-hec) applied in this study, the three-layer hydrate state does not form at r.h. <100% while, when immersing the material into liquid water, osmotic swelling sets in instantly (Rosenfeldt et al. 2016). Osmotic swelling is long-known and was first reported by U. Hofmann (Lerf 2014). It is a thermodynamically allowed repulsive process (Daab et al. 2017, 2018). Osmotic swelling in water requires careful control of temperature (Hansen et al. 2012), charge density (Daab et al. 2017), steric demand (Daab et al. 2018), and hydration enthalpy of the interlayer cation (Stöter et al. 2015). Notably, the addition of electrolytes above 0.03 mol L^{-1} or organic solvents hampers osmotic swelling (Lagaly & Ziesmer 2003). Nevertheless, swelling of clay minerals with small, neutral, organic solvent molecules is a well

* E-mail address of corresponding author: josef.breu@uni-bayreuth.de
DOI: 10.1007/s42860-019-00046-9

Electronic supplementary material The online version of this article (https://doi.org/10.1007/s42860-019-00046-9) contains supplementary material, which is available to authorized users.

documented and frequently observed phenomenon. It occurs not only with organophilized clay minerals (Lagaly et al. 2006) but also with inorganic interlayer cations (Lagaly 1984). Complexation of inorganic interlayer cations by neutral solvent molecules is driven by chemical forces like hydrogen bonding, ion-dipole interaction, coordination bonds, acid-base reactions, charge transfer, and van der Waals forces (Lagaly et al. 2006). The pioneering work of Bradley (1945) already contains a long list of complex formations of sodium and calcium interlayer cations in montmorillonite with different organic solvents. The air-dried clay samples probably contained some moisture due to the hygroscopicity of clays (Graber & Mingelgrin 1994). However, an increase in the *d* value in the 00*l*-series could be proven for any of the tested solvents. The binding of ethylene glycol and glycerol was subsequently established as a decisive test for montmorillonite (Macewan 1946; Brindley 1966). A Gutmann donor number of at least 14 was found to be a prerequisite for moving Na^+ from the hexagonal cavities toward the middle of the interlayer space (Berkheiser & Mortland 1975) while all other solvent parameters (dipole moment, dielectric constant, or surface tension) showed no correlation (Onikata et al. 1999). Reducing the cation exchange capacity from 87 to 27 meq/100 g led to no difference in crystalline swelling except for water (Berkheiser & Mortland 1975). Yamanaka et al. (1973) concluded that the strength of the interaction between cation and ligand is strictly dependent on the polarizing power of the individual interlayer ion. Bissada et al. (1967) worked out the influence of the type and charge of interlayer cations for ethanol and acetone uptake. Solvent molecules can not only be introduced to previously dried interlayer spaces but are also capable of displacing water molecules of hydrated clay minerals following the concept of hard and soft acids and bases (Lagaly et al. 2006). Anhydrous clay minerals have been swollen successfully by applying alcohols (Bissada et al. 1967; Dowdy & Mortland 1967, 1968), acetone (Bissada et al. 1967), various formamides and acetamides (Olejnik et al. 1974), dimethylsulfoxide (DMSO) (Olejnik et al. 1974), and aromatic heterocycles (Weiss 1963). More recently, clear evidence was presented that fluorohectorites show an enormous adsorption capacity even for gaseous CO_2 at room temperature (Cavalcanti et al. 2018). Brindley (1980) was, to the best of the present authors' knowledge, the only the researcher, who, up to the present day, investigated the swelling in solvent mixtures (DMSO and water). He reported osmotic swelling with Li-, Na-, and K-montmorillonite at maximum DMSO contents of 45, 30, and 10 mol.% of DMSO corresponding to 76, 63, and 30 vol.%, respectively.

MATERIALS AND METHODS

Chemicals

Acetonitrile and the 3 Å molecular sieve for drying were purchased from Sigma-Aldrich (Munich, Germany).

Synthesis of the Layered Silicate

Na-hec ($Na_{0.5}^{inter}[Mg_{2.5}Li_{0.5}]^{oct}<Si_4>^{tet}O_{10}F_2$) was obtained by melt synthesis in a closed molybdenum crucible according to a published procedure (Breu et al. 2001). The raw material was annealed for 6 weeks at 1045°C to improve intracrystalline reactivity, charge homogeneity, and phase purity, as described recently (Stöter et al. 2013).

Swelling Experiments

Na-hec was dried for 12 h at 300°C and 10^{-3} mbar and stored under argon. The solvent mixtures were prepared by adding appropriate aliquots of distilled water to carefully dried acetonitrile. Dispersions of 10 wt.% Na-hec were prepared by adding the various acetonitrile:water mixtures to dry Na-hec followed by equilibration for 5 days at room temperature (r.t.).

Small Angle X-ray Scattering (SAXS)

SAXS data were measured using the small angle X-ray system "Double Ganesha AIR" (SAXSLAB, Copenhagen Denmark). The X-ray source of this laboratory-based system is a rotating anode (copper, MicoMax 007HF, Rigaku Corporation, Tokyo, Japan) providing a micro-focused beam. The data were recorded using a position sensitive detector (PILATUS 300K, Dectris, Baden-Daettwil, Switzerland). To cover the range of scattering vectors between 0.006 and 1 $Å^{-1}$, various detector positions were used. The measurements were done in 1 mm glass capillaries (Hilgenberg, code 4007610, Malsfeld, Germany) at r.t. The circularly averaged data were normalized to incident beam, sample thickness, and measurement time before subtraction of the solvent. The subtraction was done using the approximation I(q)_dispersion-I(q)_solvent mix, which proved to be well suited in the q range discussed. The data analysis was performed with the software *Scatter* (version 2.5) (Förster et al. 2011).

Karl-Fischer (KF) Titration

KF titrations were made with a KF Coulometer 831 from Metrohm (Filderstadt, Germany), which is applicable in the region of 10 µg to 200 mg. Dispersions of 25 wt.% Na-hec were prepared in order to improve the precision. The water content of the supernatant was determined after an equilibration time of 5 days. To crosscheck for a potential influence of the concentration, a sample of 10 wt.% Na-hec in 90 vol.% acetonitrile was measured also and no significant differences were found as compared to the 25 wt.% sample.

Wide-angle Powder X-ray Diffraction (XRD)

XRD patterns of the swollen crystalline Na-hec dispersions were recorded in transmission mode on a STOE STADI P powder diffractometer (CuKα_1 radiation, Ge monochromator, DECTRIS MYTHEN 1 K strip detector, Darmstadt, Germany). The measurements were done in 1 mm glass capillaries (Hilgenberg, code 4007610, Malsfeld, Germany) at r.t.

RESULTS AND DISCUSSIONS

Phase-pure synthetic Na-hec shows uniform intracrystalline reactivity (Stöter et al. 2013) rendering it ideally suited to study swelling in more complex systems such as solvent mixtures of varying composition. Acetonitrile with a Gutmann donor number of 14.1, a dipole moment of 3.92 D, a

https://doi.org/10.1007/s42860-019-00046-9 Published online by Cambridge University Press

dielectric constant of 38.8, and a surface tension of 29.29 dyn cm^{-1} was chosen as an organic solvent and the swelling in mixtures in the range up to 35 vol.% (61 mol%) water was studied.

Na-hec does not require any purification or ion-exchange and shows a homogeneous intracrystalline reactivity. With this material at hand, swelling can be studied starting with a 1D crystalline dry powder (tactoids) all the way from crystalline to the osmotic swelling regimes simply by adding increasing amounts of the swelling medium. With water vapor applied for swelling, crystalline swelling of Na-hec is limited to the 1 WL (water layer) and 2 WL hydration states obtained at 30–70% r.h. and >90% r.h., respectively. When the water activity increased to 55 mol L^{-1} (liquid water), osmotic swelling occurred instantly. Previously, the separation of adjacent silicate layers was studied as a function of increasing volume of liquid water being added. In the initial state of swelling (Rosenfeldt et al. 2016), the separation scaled with the reciprocal volume fraction Φ^{-1} of Na-hec, which below a volume fraction of 0.0015 changed discontinuously to $\Phi^{-0.66}$ (Rosenfeldt et al. 2016). Due to the large diameter (median 20.000 nm (Stöter et al. 2013)), rotation of the individual silicate layers in dispersion is hindered and consequently the dispersions are not isotropic. At a solid content of 10 wt.% as applied in this study, rather nematic phases (Rosenfeldt et al. 2016) form as shown by interference peaks (oscillations) observed in small-angle X-ray scattering (SAXS, Fig. 1); these correspond to the very large separations of adjacent layers (>20 nm). As proposed for nontronites and montmorillonites (Michot et al. 2006), layered antimony phosphates (Gabriel et al. 2001; Davidson et al. 2018), graphene oxide (Liu et al. 2017), and titanate/niobate nanosheets (Wang & Sasaki 2014; Sano et al. 2016), the negatively charged individual Na-hec layers adopt a cofacial arrangement due to strong electrostatic repulsion.

Here the swelling was studied as a function of varying water activity. The volume of the swelling medium was kept constant, while the solvent composition (acetonitrile:water) was varied systematically over a range stretching from 65 to 100 vol.% acetonitrile.

When immersing Na-hec into the solvent mixtures, osmotic swelling of the complete material was observed up to a maximum acetonitrile content of 65 vol.% (39 mol.%). With this mixture, a separation of 252 Å was observed (Fig. 1; Fig. 2.I). As expected for a layered material, the scattering of hectorite in the osmotic swelling regime showed a q^{-2} scaling law at small and intermediate q (Stöter et al. 2015).

Applying the densities of Na-hec and this solvent mixture, the volume fraction of Na-hec in this dispersion was 3.6 vol.%. This volume fraction belongs to the first regime of osmotic swelling where the separation of adjacent silicate layers is expected to be proportional to (layer thickness)×Φ^{-1}. Assuming a thickness of 9.6 Å (≈ 1 nm) for the 2:1 silicate layer, the observed separation meets the Φ^{-1} scaling which in turn proves that all hectorite crystals were utterly delaminated and that all silicate layers were separated to the same maximum distance by the complete volume of the swelling solvent mixture available. This resembles the swelling behavior in pure water (Rosenfeldt et al. 2016) and indicates electrostatic repulsion. Apparently, because of this repulsive nature, the modulation of the electrostatics by the varying dielectric constant does not influence the layer separation.

The Φ^{-1} scaling furthermore indicated that not only the water content but the complete volume of the solvent mixture is driving the swelling to the maximum distance. At 68 vol.% acetonitrile, an osmotically swollen phase with a layer separation of 492 Å (Fig. 2.IIa) and a crystalline swollen phase with a basal spacing of 36 Å (Fig. 2.IIb) coexisted (Fig. S1). The relative proportion of the two coexisting phases cannot be determined safely by the intensities. A significant proportion of the Na-hec, however, was bound to the crystalline swelling state where less swelling agent was intercalated. The remaining solvent mixture was available for osmotic swelling of the remaining part of Na-hec. Consequently, the layer separation in the osmotically swollen phase was much larger than would be expected based on the complete Na-hec volume ratio.

In the crystalline swelling regime, the basal spacings observed are determined solely by the water activity while the solvent volume available is irrelevant. The various solvation stages represent distinct individual phases in the Gibbs sense. Transitions from one stage to the next as a function of decreasing water content of the swelling agent represent phase transitions. Cooperativity in intrinsically 2D solids is limited to two dimensions. From a thermodynamic point of view, all individual interlayers should expand or collapse at the same water activity, equilibrium might not necessarily be achieved for kinetic reasons. The materials were equilibrated at room temperature for 5 days. Nevertheless, in many cases irrational 00*l*-series were observed indicating that the two uniformly swollen phases encompassing this swelling stage occur concomitantly and randomly stacked in the tactoids. For an equilibrated material with uniform intracrystalline reactivity, plateaus with constant basal spacings over a range of compositions are expected (Stöter et al. 2015). The quasi-continuous shift of apparent basal spacings caused by random interstratification (Moore & Reynolds 1997) partially masks the plateaus and makes identification of the discrete swelling steps more difficult. The 00*l*-series were, therefore, checked carefully for rationality. According to Bailey (1982), a coefficient of variation (CV) of <0.75 indicates rationality with all interlayer spaces being swollen uniformly. Applying this criterion, six distinct solvation steps (Fig. 2.III–VIII; colored squares correspond to rational, black squares to irrational 00*l*-series) could be identified (Table 1) for 71 vol.% (Fig. S2), 78 vol.% (Fig. S3), 84 vol.% (Fig. S4), 90 vol.% (Fig. S5), 94 vol.% (Fig. 3), and 100 vol.% (Fig. S6). Note that acetonitrile and water form an azeotrope with 83.7 wt.% acetonitrile and a boiling point of 76.5°C suppressed by 5.5 K as compared to 82°C for pure acetonitrile. Consequently, the swollen samples cannot be isolated, because, upon drying, the composition of the swelling agent would inevitably change. The diffraction patterns were, therefore, recorded in transmission mode with dispersions filled into capillaries and, therefore, the tactoids were not oriented preferentially. Not surprisingly, broad humps were caused by the solvent. Most diffraction patterns showed only

https://doi.org/10.1007/s42860-019-00046-9 Published online by Cambridge University Press

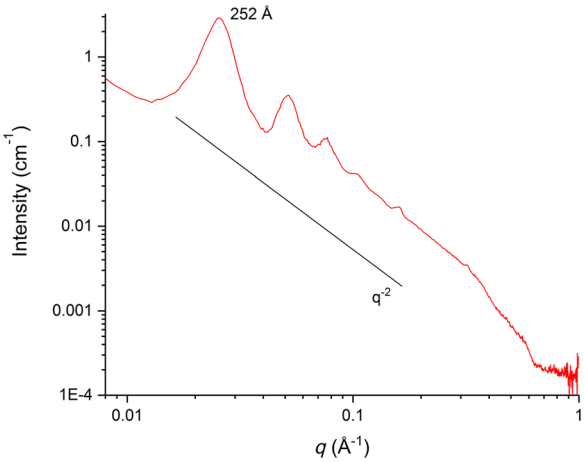

Fig 1 SAXS pattern of osmotically swollen Na-hec in 65 vol.% acetonitrile.

00*l*-reflections indicating a turbostratic stacking of the individual layers. In the diffraction patterns of samples swollen with 100 vol.% (Fig. S6), 94 vol.% (Fig. 3), and 90 vol.% (Fig. S5) acetonitrile, however, many sharp *hkl* reflections were visible, indicating partial or 3D crystalline order. Unfortunately, efforts to date to index these diffraction patterns have failed. For air-dried and anhydrous montmorillonite swollen with acetonitrile, basal spacings of 19.6 Å (Berkheiser & Mortland 1975) and ~16 Å (Muminov et al. 2006) were reported. The first agrees perfectly with the basal spacing observed at 90 vol.% acetonitrile while the latter is significantly greater than observed for 100 vol.% acetonitrile which would indicate random interstratification with higher swelling stages. The 19.6 Å basal spacing was significantly larger than values reported for 3 WL (18.7 Å) (Möller et al. 2010) which might be a first hint that this basal spacing indicates a mixed occupancy of this interlayer space by water and acetonitrile (see Table 2 and SI Section 3).

Notably, an ordered interstratification could be identified at 94 vol.% acetonitrile as indicated by a clearly visible superstructure reflection at 34.4 Å (Fig. 3, Fig. S7) followed by a rational (see red ticks in Fig. 3) series with a maximum visible order of $l = 23$. To the best of the present authors' knowledge this is the first example of a layered silicate with the same type of cation in all interlayers to be differentiated into two distinct interlayer spaces upon swelling. Ordered interstratifications for Na-hec have been reported previously for different interlayer cations being segregated into a strictly alternating sequence (Stöter et al. 2015). A partial reshuffling of Na^+ between adjacent interlayers cannot be ruled out. The fact that this phenomenon was observed with a solvent mixture, however, made it likely that the two distinct interlayer spaces differ in solvent composition. Because the basal spacing of the ordered interstratification matched perfectly with the sum of the basal spacings observed for 100 vol.% acetonitrile and 90 vol.% acetonitrile (14.8 Å + 19.6 Å = 34.4 Å), a sensible assumption is that these two phases are stacked in an ordered fashion. This would indicate that a purely acetonitrile swollen interlayer would alternate with an interlayer of mixed occupation (acetonitrile and water). The diffraction pattern of the ordered interstratification, however, cannot be explained by a superposition of the patterns of 33.3 Å tactoids with 71 vol.% acetonitrile and 19.6 Å tactoids with 90 vol.% acetonitrile. Moreover, given thermodynamic control, these two largely separated phases cannot coexist in equilibrium (Fig. S8).

While the sequence of swelling could be followed easily by X-ray diffraction, conclusive experimental evidence regarding the composition of the interlayer space (or, in the case of the

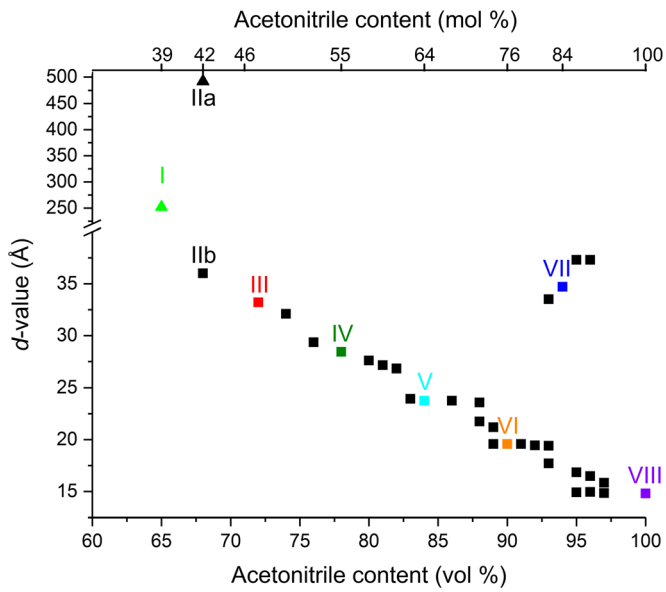

Fig. 2 Series of rational (colored marks) and irrational (black marks) *d* values of swollen Na-hec depending on the applied acetonitrile:water ratio. Osmotically swollen phases are marked with ▲, crystalline swollen phases are shown as ■. Roman numerals describe compositions discussed in the main text.

https://doi.org/10.1007/s42860-019-00046-9 Published online by Cambridge University Press

Table 1 *d* values and coefficient of variation (CV) for various solvent mixtures of acetonitrile and water with Na-hec.

Vol.% acetonitrile	Mol.% acetonitrile	Basal spacing (Å)	CV (%)
71	46	33.3	0.16
78	55	28.5	0.03
84	64	23.8	0.06
90	76	19.6	0.24
94	84	34.4	0.34
100	100	14.8	0.26

94 vol.% sample, the two different interlayer spaces) cannot be obtained. While for hydrated interlayer spaces structural models exist based on single-crystal structure refinements and on molecular dynamics simulations (Ferrage et al. 2005), no such reliable evidence exists in the literature for acetonitrile or mixed occupied interlayers. Theoretical calculations suggested that acetonitrile coordinates octahedrally to Na^+ (Spangberg & Hermansson 2004). A coordination of one acetonitrile molecule per Na^+ was shown experimentally to be retained in montmorillonite even in vacuum (10^{-2} mm Hg) (Dios-Cancela et al. 2000), suggesting a significant binding energy. Moreover, Na^+ was found to be solvated preferably by acetonitrile in acetonitrile:water mixtures (Hawlicka 1987). These observations might suggest a preference of acetonitrile over water also to interlayer Na^+. Applying Karl-Fischer titrations of the supernatants, however, proved clearly an enrichment of acetonitrile as compared to the starting composition (Table 2). This would indeed suggest a greater selectivity of water over acetonitrile for the interlayer space. To improve the analytical precision of these experiments, equilibration was done at a greater Na-hec concentration (25 wt.%). As indicated above, the observed basal spacing at 90 vol.% acetonitrile cannot be explained by hydration but indicates a mixed solvent uptake. Generally, observed basal spacings and solvent ratios of the supernatant can only be explained consistently if a concomitant adsorption of both acetonitrile and water is postulated.

Unfortunately, the total adsorption capacities could not be determined reliably because removal of surface-adsorbed solvents and intercalated solvent overlaps and the azeotropic behavior modulates the latter. With a few simple and well justified assumptions, nevertheless, a semi-quantitative analysis can be deduced (see SI Section 3 and Table S1 for details). In short, first the adsorbed volume per unit cell (a = 5.2401(10) Å, b = 9.0942(10) Å) (Breu et al. 2003) was calculated from the observed basal spacing. This volume was then subtracted from the total volume of the swelling solvent. Taking into account the water content determined experimentally and the density (Fig. S9) of the supernatant, the absolute volumes of acetonitrile and water in the supernatant were calculated, which correlate with the adsorbed volumes of both solvents. These were normalized to a gram of Na-hec (Table 2). With all solvent mixtures applied for swelling, both acetonitrile and water were intercalated into the interlayer space. Even though a surplus of water would be available, its selectivity for adsorption is never sufficient that acetonitrile could not compete in significant amounts. The selectivity for water, however, rose steadily with increasing water content of the swelling solvent. The amount of acetonitrile and water adsorbed at 94 vol.%, resulting in an ordered interstratified structure which, corresponded well with the arithmetic mean of the 90 vol.% and 100 vol.% samples (see SI Section 4 for details) which gave further support for a strictly alternating structure of pure

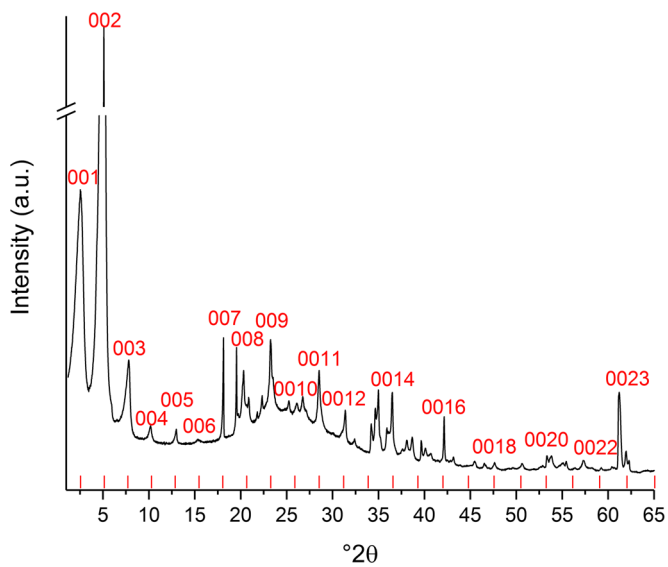

Fig. 3 Ordered interstratification of two different solvent compositions in Na-hec using 94 vol.% acetonitrile. Theoretical 00*l* peak positions and indexed 00*l* peaks are displayed in red.

https://doi.org/10.1007/s42860-019-00046-9 Published online by Cambridge University Press

Table 2 Calculated solvent adsorption capacities of Na-hec in the respective acetonitrile:water mixtures and their adsorbed water:acetonitrile molar ratio.

Acetonitrile content	71 vol.%	78 vol.%	84 vol.%	90 vol.%	94 vol.%
Acetonitrile capacity (mmol g^{-1})	9.0	7.6	6.0	5.2	4.5
Water capacity (mmol g^{-1})	23.8	17.9	12.5	6.0	2.9
Water : acetonitrile ratio	2.6	2.4	2.1	1.2	0.6
Total capacity (mmol g^{-1})	32.8	25.5	18.5	11.2	7.4

acetonitrile interlayers (3.7 mmolg^{-1} acetonitrile) and the interlayer composition of the 90 vol.% sample (5.2 mmol g^{-1} acetonitrile and 6.0 mmol g^{-1} water).

CONCLUSION

Crystalline swelling of Na-hec in aqueous acetonitrile yielded well defined solvates with giant basal spacings (33.3 Å) as compared to swelling in pure water. The resulting interlayer height was larger than most organic molecules. Preliminary results showed that this eases kinetic hindrance, e.g. when exchanging Na^+ for large organic or metal-organic pillars as needed in the synthesis of MOPS (Bärwinkel et al. 2017; Herling et al. 2018; Rieß et al. 2018). The most surprising result was certainly the formation of an ordered interstratification based on different compositions of neutral solvent molecules in the interlayer space. The future will show if this is a general phenomenon in solvent mixtures. If adding a second swelling agent already induces such dramatic changes in the swelling behavior, extending swelling studies into ternary solvent compositions will, of course, be most interesting. Work in that direction is in progress.

ACKNOWLEDGMENTS

The authors thank Birgitta Brunner for performing the Karl-Fischer titrations. The authors also acknowledge the financial support of this work by the Deutsche Forschungsgemeinschaft (SFB 840 and SFB 1357).

COMPLIANTS WITH ETHICAL STANDARDS

Conflict of Interest

The authors declare that they have no conflict of interest.

REFERENCES

Bailey, S. W. (1982). Nomenclature for regular interstratifications. *American Mineralogist, 67*, 394–398.

Bärwinkel, K., Herling, M. M., Rieß, M., Sato, H., Li, L. C., Avadhut, Y. S., Kemnitzer, T. W., Kalo, H., Senker, J., Matsuda, R., Kitagawa, S., & Breu, J. (2017). Constant volume gate-opening by freezing rotational dynamics in microporous organically pillared layered silicates. *Journal of the American Chemical Society, 139*, 904–909.

Berkheiser, V., & Mortland, M. M. (1975). Variability in exchange ion position in smectite — dependence on interlayer solvent. *Clays and Clay Minerals, 23*, 404–410.

Bissada, K. K., Johns, W. D., & Cheng, F. S. (1967). Cation-dipole interactions in clay organic complexes. *Clay Minerals, 7*, 155–166.

Bradley, W. F. (1945). Molecular associations between montmorillonite and some polyfunctional organic liquids. *Journal of the American Chemical Society, 67*, 975–981.

Breu, J., Seidl, W., Stoll, A. J., Lange, K. G., & Probst, T. U. (2001). Charge Homogeneity in Synthetic Fluorohectorite. *Chemistry of Materials, 13*, 4213–4220.

Breu, J., Seidl, W., & Stoll, A. J. (2003). Fehlordnung bei Smectiten in Abhängigkeit vom Zwischenschichtkation. *Zeitschrift für anorganische und allgemeine Chemie, 629*, 503–515.

Brindley, G. W. (1966). Ethylene glycol and glycerol complexes of smectites and vermiculites. *Clay Minerals, 6*, 237–259.

Brindley, G. W. (1980). Intracrystalline swelling of montmorillonites in water–dimethylsulfoxide systems. *Clays and Clay Minerals, 28*, 369–372.

Cavalcanti, L. P., Kalantzopoulos, G. N., Eckert, J., Knudsen, K. D., & Fossum, J. O. (2018). A nano-silicate material with exceptional capacity for CO2 capture and storage at room temperature. *Scientific Reports, 8*.

Daab, M., Rosenfeldt, S., Kalo, H., Stöter, M., Bojer, B., Siegel, R., Forster, S., Senker, J., & Breu, J. (2017). Two-step delamination of highly charged, vermiculite-like layered silicates via ordered heterostructures. *Langmuir, 33*, 4816–4822.

Daab, M., Eichstaedt, N. J., Edenharter, A., Rosenfeldt, S., & Breu, J. (2018). Layer charge robust delamination of organo-clays. *RSC Advances, 8*, 28797–28803.

Davidson, P., Penisson, C., Constantin, D., & Gabriel, J. C. (2018). Isotropic, nematic, and lamellar phases in colloidal suspensions of nanosheets. *Proceedings of the National Academy of Sciences, 115*, 6662–6667.

Dazas, B., Lanson, B., Breu, J., Robert, J. L., Pelletier, M., & Ferrage, E. (2013). Smectite fluorination and its impact on interlayer water content and structure: A way to fine tune the hydrophilicity of clay surfaces? *Microporous and Mesoporous Materials, 181*, 233–247.

Devineau, K., Bihannic, I., Michot, L., Villieras, F., Masrouri, F., Cuisinier, O., Fragneto, G., & Michau, N. (2006). In situ neutron diffraction analysis of the influence of geometric confinement on crystalline swelling of montmorillonite. *Applied Clay Science, 31*, 76–84.

Dios-Cancela, G., Alfonso-Mendez, L., Huertas, F. J., Romero-Taboada, E., Sainz-Diaz, C. I., & Hernandez-Laguna, A. (2000). Adsorption mechanism and structure of the montmorillonite complexes with (CH3)(2)XO (X = C, and S), (CH3O)(3)PO, and CH3-CN molecules. *Journal of Colloid and Interface Science., 222*, 125–136.

Dowdy, R. H., & Mortland, M. M. (1967). Alcohol–water interactions on montmorillonite surfaces. I. Ethanol. *Clays and Clay Minerals, 15*, 259–271.

Dowdy, R. H., & Mortland, M. M. (1968). Alcohol-water interactions on montmorillonite surfaces. II. Ethylene glycol. *Soil Science, 105*, 36–43.

Ferrage, E., Lanson, B., Sakharov, B. A., & Drits, V. A. (2005). Investigation of smectite hydration properties by modeling experimental x-ray diffraction patterns: Part I. Montmorillonite hydration properties. *American Mineralogist, 90*, 1358–1374.

https://doi.org/10.1007/s42860-019-00046-9 Published online by Cambridge University Press

Förster, S., Fischer, S., Zielstke, K., Schellbach, C., Sztucki, M., Lindner, P., & Perlich, J. (2011). Calculation of scattering-patterns of ordered nano- and mesoscale materials. *Advances in Colloid and Interface Science, 163*, 53.83.

Gabriel, J. C., Camerel, F., Lemaire, B. J., Desvaux, H., Davidson, P., & Batail, P. (2001). Swollen liquid-crystalline lamellar phase based on extended solid-like sheets. *Nature, 413*, 504–508.

Graber, E. R., & Mingelgrin, U. (1994). Clay swelling and regular solution theory. *Environmental Science & Technology, 28*, 2360–2365.

Hansen, E. L., Hemmen, H., Fonseca, D. M., Coutant, C., Knudsen, K. D., Plivelic, T. S., Bonn, D., & Fossum, J. O. (2012). Swelling transition of a clay induced by heating. *Scientific Reports*, *2*.

Hawlicka, E. (1987). Self-diffusion of sodium, chloride and iodide-ions in acetonitrile-water mixtures. *Zeitschrift für Naturforschung B, 42*, 1014–1016.

Herling, M. M., Rieß, M., Sato, H., Li, L. C., Martin, T., Kalo, H., Matsuda, R., Kitagawa, S., & Breu, J. (2018). Purely physisorption-based co-selective gate-opening in microporous organically pillared layered silicates. *Angewandte Chemie International Edition, 57*, 564–568.

Hofmann, K., Endell, K., & Wilm, D. (1933). Kristallstruktur und Quellung von Montmorillonit. *Zeitschrift für Kristallographie - Crystalline Materials, 86*, 1–6.

Kalo, H., Milius, W., & Breu, J. (2012). Single crystal structure refinement of one- and two-layer hydrates of sodium fluorohectorite. *RSC Advances, 2*, 8452–8459.

Lagaly, G. (1984). Clay-organic interactions. *Philosophical Transactions of the Royal Society A, 311*, 315–332.

Lagaly, G., Ogawa, M., & Dékány, I. (2006). Chapter 7.3 clay mineral organic interactions. *Developments in Clay Science, 1*, 309–377.

Lagaly, G., & Ziesmer, S. (2003). Colloid chemistry of clay minerals: The coagulation of montmorillonite dispersions. *Advances in Colloid and Interface Science, 100–102*, 105–128.

Lerf, A. (2014). Storylines in intercalation chemistry. *Dalton Transactions, 43*, 10276–10291.

Liu, Y., Xu, Z., Gao, W., Cheng, Z., & Gao, C. (2017). Graphene and other 2D colloids: Liquid crystals and macroscopic fibers. *Advanced Materials, 29*, 1606794.

Macewan, D. M. C. (1946). The identification and estimation of the montmorillonite group of minerals, with special reference to soil clays. *Journal of the Society of Chemical Industry, 65*, 298–304.

Madsen, F. T., & Müller-Vonmoos, M. (1989). The swelling behaviour of clays. *Applied Clay Science, 4*, 143–156.

Marry, V., Dubois, E., Malikova, N., Durand-Vidal, S., Longeville, S., & Breu, J. (2011). Water dynamics in hectorite clays: Infuence of temperature studied by coupling neutron spin echo and molecular dynamics. *Environmental Science & Technology, 45*, 2850–2855.

Michot, L. J., Bihannic, I., Maddi, S., Funari, S. S., Baravian, C., Levitz, P., & Davidson, P. (2006). Liquid-crystalline aqueous clay suspensions. *Proceedings of the National Academy of Sciences, 103*, 16101–16104.

Möller, M. W., Handge, U. A., Kunz, D. A., Lunkenbein, T., Altstädt, V., & Breu, J. (2010). Tailoring shear-stiff, mica-like nanoplatelets. *ACS Nano, 4*, 717–724.

Mooney, R. W., Keenan, A. G., & Wood, L. A. (1952). Adsorption of water vapor by montmorillonite. II. Effect of exchangeable ions and lattice swelling as measured by X-ray diffraction. *Journal of the American Chemical Society, 74*, 1371–1374.

Moore, D. M., & Reynolds, R. C. (1997). *X-ray diffraction and the identification and analysis of clay minerals* (2nd ed.). New York: Oxford University Press.

Muminov, S. Z., Gulyamova, D. B., & Pribylov, A. A. (2006). Adsorption of acetonitrile vapor on sodium and polyhydroxyaluminum montmorillonites. *Colloid Journal, 68*, 584–587.

Norrish, K. (1954). The swelling of montmorillonite. *Discussions of the Faraday Society, 18*, 120–134.

Olejnik, S., Posner, A. M., & Quirk, J. P. (1974). Swelling of montmorillonite in polar organic liquids. *Clays and Clay Minerals, 22*, 361–365.

Onikata, M., Kondo, M., & Yamanaka, S. (1999). Swelling of formamide-montmorillonite complexes in polar liquids. *Clays and Clay Minerals, 47*, 678–681.

Rieß, M., Senker, J., Schobert, R., & Breu, J. (2018). Microporous organically pillared layered silicates (mops): A versatile class of functional porous materials. *Chemistry – A European Journal, 24*, 1–10.

Rosenfeldt, S., Stöter, M., Schlenk, M., Martin, T., Albuquerque, R. Q., Förster, S., & Breu, J. (2016). In-depth insights into the key steps of delamination of charged 2d nanomaterials. *Langmuir, 32*, 10582–10588.

Sano, K., Kim, Y. S., Ishida, Y., Ebina, Y., Sasaki, T., Hikima, T., & Aida, T. (2016). Photonic water dynamically responsive to external stimuli. *Nature Communications, 7*, 1–9.

Spangberg, D., & Hermansson, K. (2004). The solvation of Li^+ and Na^+ in acetonitrile from ab initio-derived many-body ion-solvent potentials. *Chemical Physics, 300*, 165–176.

Stöter, M., Kunz, D. A., Schmidt, M., Hirsemann, D., Kalo, H., Putz, B., Senker, J., & Breu, J. (2013). Nanoplatelets of sodium hectorite showing aspect ratios of approximate to 20 000 and superior purity. *Langmuir, 29*, 1280–1285.

Stöter, M., Rosenfeldt, S., & Breu, J. (2015). Tunable exfoliation of synthetic clays. *Annual Review of Materials Research, 45*, 129–151.

Viani, B. E., Low, P. F., & Roth, C. B. (1983). Direct measurement of the relation between interlayer force and interlayer distance in the swelling of montmorillonite. *Journal of Colloid and Interface Science, 96*, 229–244.

Wang, L., & Sasaki, T. (2014). Titanium oxide nanosheets: Graphene analogues with versatile functionalities. *Chemical Reviews, 114*, 9455–9486.

Weiss, A. (1963). Organische Derivate der glimmerartigen Schichtsilicate. *Angewandte Chemie Inte rnational Edition, 75*, 113–122.

Yamanaka, S., Kanamaru, F., & Koizumi, M. (1973). Role of interlayer cations in the formation of acrylonitrile-montmorillonite complexes. *The Journal of Physical Chemistry A, 78*, 42–44.

You, S. J., Kunz, D., Stöter, M., Kalo, H., Putz, B., Breu, J., & Talyzin, A. V. (2013). Pressure-induced water insertion in synthetic clays. *Angewandte Chemie International Edition, 52*, 3891–3895.

(Received 31 July 2019; revised 12 November 2019; AE: M. Ogawa)